Unified All-scale Potential for Positive and Negative Mass: Negative Mass Behavior

Judith A. Giannini

Retired, Bellefonte, PA 16823, USA

Email: jag.cck@gmail.com

Abstract: The Standard Model faces challenges in its attempts to explain dark matter and dark energy. The Fractal Rings and Composite Elementary Particles (FRACEP) model was developed as an alternative that might shed some light on the problem. It is based on both positive and negative mass fundamental particles ($\mathcal{G}p$ and $\mathcal{G}n$ respectively), and it includes a fully unified potential (V_{FRACEP}) to characterize the behavior of positive and negative mass sources. This potential is a function of mass and the square-root of mass, giving it both real and imaginary components at every scale for negative mass sources. The real component at the macro-scale far-field is consistent with Newton for positive or negative mass sources before a near-field transition to oscillation. The near-field oscillation for the $\mathcal{G}n$-$\mathcal{G}p$ interaction quickly grows to the large, repulsive level expected for a creation event, a condition that might have driven an inflationary expansion of space in the early universe. The behavior of the negative-source potential might help explain some of the dark matter and energy puzzle.

Keywords: negative mass, negative energy, alternate gravity, composite elementary particles, cosmic inflation.

1. Introduction

The Lao Tse (Tao-Te-Ching) tells the Chinese wisdom about the nature of the Universe: the "being" and the "non-being" where "these two spring from the same source" – "the Darkness within the Darkness, the gate to all mystery" [1]. Although Lao Tzu's words are ancient, they sound strangely reminiscent of the modern puzzle of dark matter and energy and their relation to the "Bright Universe" we see (the "being"). They hint of a "Dark Universe" we cannot see (the "non-being" – the unseen dark matter and energy within the darkness of the cosmos).

About a thousand years later, Newton [2] reflected on the fact that we gain information about matter through observations by our senses, and, that knowledge (of "sensible bodies") might then be applied universally to all bodies. But, he cautioned that there are bodies beyond the range of our senses, perhaps inferring the existence of the sub-atomic world that was not obvious. However, like the Tao-Te-Ching, his statement may be aptly prophetic about the possibility of negative matter.

Newton's theory of gravitation is remarkably successful at characterizing the behavior of attracting bodies from every-day scales on Earth to planetary scales, but with some limitations. In the early 1920s, Einstein's general theory of relativity changed the way gravitational interactions were viewed – from the action-at-a-distance pull between two mass-containing bodies to a field-oriented view based on the warping of space by the presence of the masses. General relativity resolved Newton's limitations and more – providing the basis of modern day cosmology. Its cosmological constant (used by Einstein to balance his equations) allowed a model of the expanding universe with the first concept of dark energy (DE). In 1997, Perlmutter et al. [3] presented evidence for accelerating expansion in the universe that was assumed to be the result of DE. There are a variety of candidates for DE, but, the nature of that phenomenon is still unclear [4].

In the late 1930's, cosmological models discovered a problem with their estimates of the amount of mass contained in the universe (a determinant of the expansion state). It was found that insufficient mass, based on the amount of observed visible mass, implied many systems that appeared stable should be gravitationally unbounded [5]. The proposed solution to the missing mass problem was the hypothesis of dark (unseen) matter (DM). Although the nature of DM was unknown, increasing galaxy and nebula masses with this unseen matter, allowed the theory and observations to agree. Burbidge [6] cautioned that the results of this addition were strongly dependent on the assumptions used in the theory.

In 1983, Milgram proposed a modification to Newton's laws (MOND) that allowed the rotation rates (for some galaxies) to be satisfied without DM [7] – a theory that is still hotly contested. The predominating consensus of cosmologists, today, is the DM and DE paradigm [8]. The contents of the universe by this paradigm are divided as: DE (dark energy, identity unknown), ~73%; DM (identity unknown), ~23%; other non-luminous matter (gasses, neutrinos and super massive black holes) and luminous matter (stars, gasses and radiation), ~4%. Numerous possible candidates have been proposed for DM [9]. WIMPS and axions are the most favored ones, though, to date, the search for WIMPS has not been successful and some circles are pinning hopes on axion detection [10]. There is a growing interest in primordial black holes as a possible source of DM [11-12], as well as, the possibility of identifying DM at Fermi scales [13-14].

Chardin and Manfredi [15] considered the symmetric matter-anti-matter Dirac-Milne universe as an analog of the electron-hole system in a semiconductor as a possible relation of DM to negative mass. Barghout [16, 17] considers modifications to Newtonian dynamics that manifest themselves as DM and DE.

In [18], Chang extended Dirac's theory to develop the field equations leading to four types of matter: positive matter, positive anti-matter, negative matter and negative anti-matter. He further considered the nature of negative matter as DM at cosmic scales and some possible tests of the concept [19, 20].

Petite and his colleagues [21] developed the Janus cosmological model of the universe which is based on Einstein's equations. However, it considers the interaction of positive and negative masses where the two types of matter have different light speed. Their twin-universe system of coupled equations shows like-mass-types attracting and unlike-mass-types repelling, and includes both positive-energy photons and negative-energy photons. In a non-steady state solution [22], they address the possibility of negative matter clumping, the nature of DE and its relation to expansion in the universe.

As an alternative, the Fractal Rings and Composite Elementary Particles (FRACEP) model [23] develops composite versions of the Standard Model (SM) quarks, leptons and bosons (the "Bright Universe") having mostly positive mass. This model leads to an additional set of particles (the "Dark Universe") having mostly negative mass, that might provide some options in the DM search.

In FRACEP's dual universe, the mass-types interact like the Petit-model masses, and it contains four types of matter like the Chang model. Unlike the other models, FRACEP considers the mixed-mass-type internal structure of its particles, proposing an explanation of quark and lepton instability and half-life decay. The mathematical basis for FRACEP's construction is under development.

A fully unified potential (V_{FRACEP}) was developed that was intended to describe the FRACEP particles' behavior. Its development assumed a single unified force governs matter interactions at all scales. Its functional form was empirically derived from known positive mass forces at the macro scale (Newton) and at the quantum scale (neutron scattering [24]). The philosophy considers the quantum scale behavior to be a manifestation of small-scale interactions of the unified force of nature.

An earlier work [25] focused on the positive mass results. This paper describes the mathematical form of the unified potential, and compares the negative source potential with the positive source potential results.

2. The FRACEP Potential (V_{FRACEP})

V_{FRACEP} addresses Planck-length scales to the largest cosmic scales. It characterizes both positive-mass and negative-mass sources. In its most general form, it is a function of both time and space, $V_{FRACEP} = F(\mathrm{t}) \cdot V(r)$. The $F(\mathrm{t})$ describes temporal behavior important to the decay times of fermions, and the oscillation frequencies associated with charge and spin characteristics of FRACEP's charge-carriers and spin-carriers. This work considers only the spatial behavior, $V_{FRACEP} = V(r)$.

V_{FRACEP}'s functional form was determined by empirically matching (as described in [25]) the behavior of V_N at macro scales, and the neutron-neutron scattering potential, in [24], at quantum scales. This characterizes positive-source masses down to V_{FRACEP}'s smallest possible separation distance $r = 3.3\text{x}10^{-20}$ fm, the classical radius of its fundamental particles, $\mathcal{G}p$ and $\mathcal{G}n$.

The negative-source mass behavior, has some similarities, but also some differences from that of the positive source and is a direct result of the functional form needed to produce a unified function over all scales for the positive-source mass.

The mathematical form of V_{FRACEP} is:

$$V_{FRACEP} = m_t \left[A_0(M) + B_0(\sqrt{M})\right] \sin\left[S(r, M) + T(r, \sqrt{M})\right] E_0(r, M); \qquad (1a)$$

$$A_0 = 1 / (0.18\, M),$$
$$B_0 = 9.2095\times10^{-8}\, \sqrt{M},$$
$$E_0 = \exp\{-2.4\, r\, |M| / [M^2 + (m_{\mathcal{G}p}/m_\pi)]\}; \qquad (1b)$$

$$S(r, M) = K_1 + K_f,$$
$$K_1 = -150\, (\pi/180)\, 0.09\, (r/M)^2\, E_1,$$
$$E_1 = \exp[-67\, (m_{\mathcal{G}p}/m_\pi) / |M|],$$

$$K_f = -(\pi/180)\ 0.000092\ [M / 8\times10^{60}]^2\ [1.496\times10^{26}/\mathrm{r}]^3; \tag{1c}$$

$$\begin{aligned} T(r, \sqrt{M}) &= K_2 + K_3 + K_4, \\ K_2 &= -150\ (\pi/180)\ (0.00006/m_\pi)\ \sqrt{M} / r, \\ K_3 &= 150\ (\pi/180)\ E_1 / \sqrt{M}, \\ K_4 &= K_3 / r. \end{aligned} \tag{1d}$$

$M = m_s / m_\pi$ where m_s is the source mass for which the potential is computed, $m_\pi = 139.57$ MeV/c^2 (the mass of the pi-meson). The m_t is the responding test mass, and $m_{Gp} = 1.72\times10^{-22}$ MeV/c^2 (the mass of Gp). The calculation units are: masses in MeV/c^2, r in fermis, and V_{FRACEP} in MeV. The macro-scale conversion to these units are: 1.7826915×10^{-33} MeV/c^2 per kg; 1.0×10^{15} fm/m; 1.496×10^{11} m/AU; 1.6022×10^{-13} J/MeV; 63240 AU/ltyr; 1 SU = 1.99×10^{30} kg.

$T(r, \sqrt{M})$ becomes imaginary when M is negative because of the $\sqrt{M}$ factor in (1d), giving V_{FRACEP} an imaginary component. This is not true of V_N which is always real, retaining the same function but changing sign. We assume an absolute value for M in E_0 and E_1 to guarantee V_{FRACEP} decays at large distances for $M < 0$. For M < 0, the sine function is expressed as:

$$\sin(S + i\ T) = [\sin(S) \cosh(T)] + [\cos(S)\ i \sinh(T)]. \tag{2}$$

This gives:

$$\begin{aligned} V_{FRACEP}\ (M < 0) = {} & m_t\, E_0(r, M)\ \{[A_0 \sin(S) \cosh(T) - B_0 \cos(S) \sinh(T)] \\ & + \ i\ [A_0 \cos(S) \sinh(T) + B_0 \sin(S) \cosh(T)]\ \} \end{aligned} \tag{3}$$

The result of this change is not a simple redistribution of the value of V_N between the real and imaginary parts of V_{FRACEP}.

3. V_{FRACEP} Macro Scale Behavior

The macro-scale behavior of gravity is very wide-ranged, affecting everything from tiny masses at micrometer separations to large astronomical bodies at cosmic scales. V_{FRACEP} allows for the computation of the potential for both positive and negative source masses for all of these cases with a single multi-term function. At macro scales, the dominating terms are the K_2 (1d) and K_f (1c). In all cases, the positive m_s has a zero imaginary part, while, the negative m_s has both real and imaginary parts. By comparison, the V_N is totally real regardless of the sign of the source.

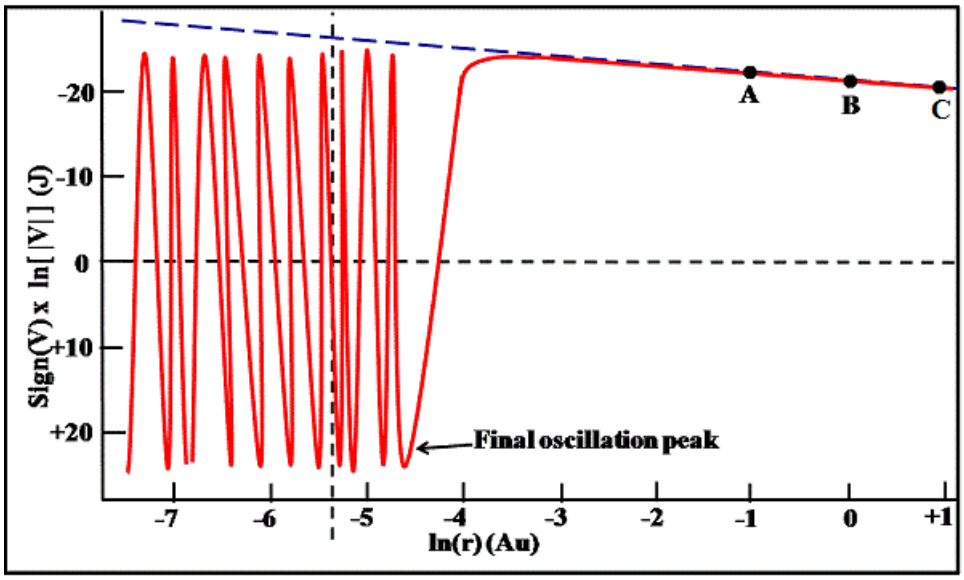

FIGURE 1. Shown is the characteristic behavior for all macro-scale positive-mass sources. The solid red line is V_{FRACEP} and the broken blue line is V_N. The vertical dashed line indicates the sun's radius, at 0.0047 AU. A indicates inside Mercury's orbit at 0.378 AU, B is Earth's orbit at 1 AU, and C is the asteroid Ceres orbit at 2.77 AU. (m_s = +1Su = 1.99×10^{30} kg, and m_t = 1 kg).
Note that all computations here assume approximately point sources; and, real world computations would require the usual application of finite-element-like techniques.

V_{FRACEP} has the $1/r$ fall-off and the same sign as V_N (for $M > 0$ and for the real part when $M < 0$) at macro scales in the "main region" where m_s and m_t are sufficiently separated. In the "near-field transition region", where m_s and m_t are much closer together, V_{FRACEP} shows a non-Newtonian oscillation for both positive and negative sources. For $M < 0$, the imaginary part generally decays more quickly at the larger r, and transitions to oscillation at smaller r before the real part. At the smallest macro-scale masses, this latter region corresponds to a transition from gravity-like to quantum-like behavior. Similarly, at the largest masses (e.g., for black hole-type masses, and even for Sun-like masses), the near-field region shows quantum-like behavior as well. The non-synchronized oscillation in V_{FRACEP}'s two components might result in a negative tidal-like force (as described by Barghout [16]) giving a longer range effect at galactic scales than in immediately obvious. This possibility requires further study.

Figure 1 shows an example of the V_{FRACEP} behavior at macro scales for a positive m_s. In this case, m_s = +1 SU (the mass of the Sun) at solar system distances. The figure shows perfect agreement with V_N in the "main region" before beginning an oscillatory transition to quantum-like behavior (at the final oscillation peak) [26]. This is typical behavior for all positive source masses from for the smallest kg-sized masses through the largest cosmic masses.

Figure 2 shows how the behavior of V_{FRACEP} changes when the m_s becomes negative. Here, m_s = –1SU at solar system distances, and the figure shows the real part (V_{FRACEP}-R) and the imaginary part (V_{FRACEP}-I) compared to V_N.

For the "near-field transition region" (a), both V_{FRACEP}-R and V_{FRACEP}-I have a decaying oscillation not seen in V_N, but approximately bounded by V_N. For the "main region" (b), V_{FRACEP}-R agrees exactly in amplitude and sign (repulsive) with V_N before showing signs of beginning to diverge at the smallest r. V_{FRACEP}-I, on the other hand, has flipped sign (becoming attractive) and has a smaller amplitude, but a more rapid fall-off. This behavior is typical for all macro-scale masses – though the details of the fall-off rate and relative amplitudes vary. For comparison, Table 1 summarizes the variations for a larger and a smaller mass.

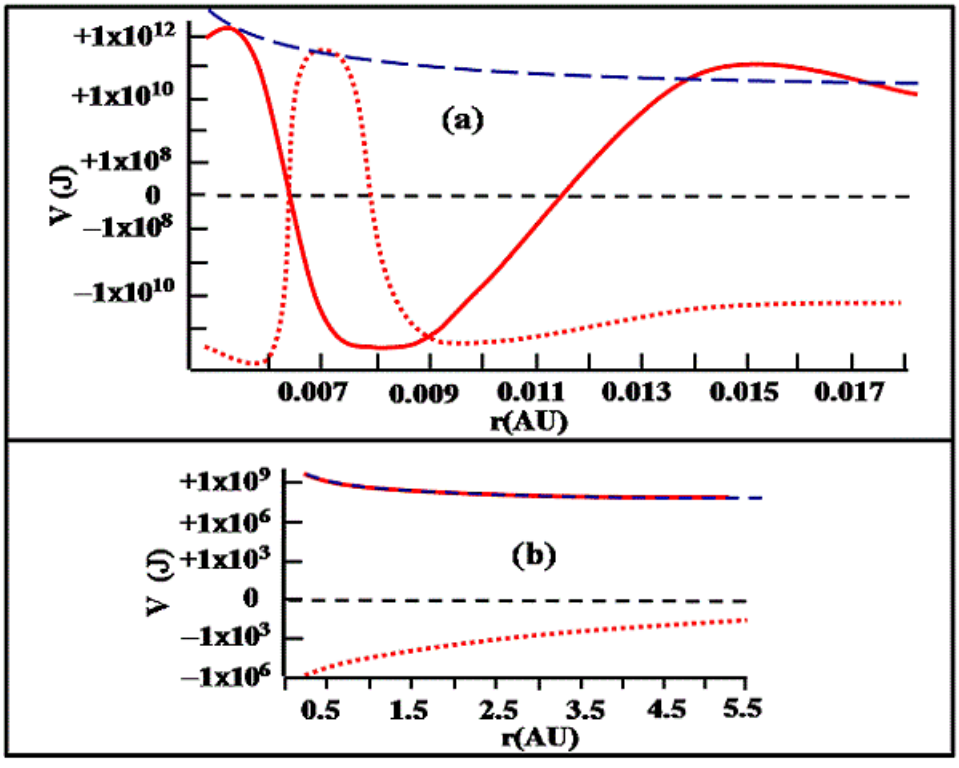

FIGURE 2. Shown is the characteristic behavior for all macro-scale negative-mass sources. The solid red line is the real part, V_{FRACEP}-*R*, and the dotted red line is the imaginary part, V_{FRACEP}-*I*. The broken blue line is V_N. At smaller *r* (a), both V_{FRACEP}-*R* and V_{FRACEP}-*I* oscillate (like the positive source potential, in Fig. 1). At larger *r* (b), V_{FRACEP}-*R* equals V_N, but, V_{FRACEP}-*I* changes sign, and is only ~0.05% of V_N at 0.378 AU. It decreases to ~0.008% of V_N by Earth's orbit. In this case, before going into oscillation, V_{FRACEP}-*R* is repulsive (like V_N) while V_{FRACEP}-*I* is attractive. (m_s = –1Su, and m_t = +1 kg).

4. V_{FRACEP} Quantum Scale Behavior

The quantum scale of interest spans from about composite particles such as pi-mesons (m_π = 139.57 MeV/c^2) to FRACEP's smallest fundamental particles, *Gp* and *Gn*. ($\pm$1.72×10^{-22} MeV/c^2). V_{FRACEP} characterizes the quantum-scale behavior by empirically matching the Standard Model nuclear potential for neutron-neutron scattering (which assumes all positive mass) based on pi-meson

exchange (OPED model) within the valid range of that model (~0.5 fm to ~2.5 fm) [24].

TABLE 1. This summarizes results for V_{FRACEP} at two macro-scale source masses bracketing the solar system results in Fig.1 and Fig. 2. (for both positive m_s and negative m_s). V_N in each region is given for comparison. For the 55 kg cases, range is in meters; and, for the $2x10^6$ SU, range is in light-years.

Mass	**+55 kg**	**–55 kg**	**+2x10^6 SU**	**–2x10^6 SU**
Near-field Transition Region				
Range	5×10^{-16} to 5×10^{-4}	5×10^{-8} to 4×10^{-4}	1×10^{-5} to 1.0	1×10^{-5} to 1.0
V_N(J)	-10^{7} to -10^{-5} 1/r decay	10^{-1} to 10^{-5} 1/r decay	-10^{15} to -10^{10} 1/r decay	10^{15} to 10^{10} 1/r decay
V_F(J) **Real**	$\pm10^{-4}$ Oscillating	10^{141} to 10^{-5} Decay to 1/r by 4×10^{-5}	$\pm10^{14}$ to -10^{10} Osc. decay to 1/r by 10^{-1}	$\pm10^{34}$ to $+10^{10}$ Osc. decay to 1/r by 6×10^{-3}
V_F(J) **Imag**	0.0	-10^{132} to -10^{-23} Non-1/r decay	0.0	$\pm10^{34}$ to $\pm10^{6}$ Osc. decay.
Main Region				
Range	5×10^{-5} to $9\times10^{+3}$	5×10^{-5} to $9\times10^{+3}$	1.0 to 9×10^{4}	1.0 to 9×10^{4}
V_N(J)	-10^{-4} to -10^{-13} 1/r decay	10^{-4} to 10^{-13} 1/r decay	-10^{10} to -10^{5} 1/r decay	10^{10} to 10^{5} 1/r decay
V_F(J) **Real**	-10^{-4} to -10^{-13} 1/r decay	10^{-4} to 10^{-13} 1/r decay	-10^{10} to -10^{5} 1/r decay	10^{10} to 10^{5} 1/r decay
V_F(J) **Imag**	0.0	-10^{-20} to -10^{-31} Non-1/r decay	0.0	-10^{6} to -10^{-9} Non-1/r decay

At quantum scales, V_{FRACEP} characterizes both positive m_s and negative m_s, where the dominating terms are the K_1 (1c), and K_3 and K_4 (1d). As the r increases, the K_1 and K_4 terms reverse rolls in their dominance. Like the macro-scale cases, V_{FRACEP} for positive m_s is totally real, while for negative m_s, it has both real and imaginary parts. OPED is totally real.

Figure 3 shows an example of the V_{FRACEP} behavior at quantum scales for a positive m_s. In this case with the pi-meson source, V_{FRACEP} shows reasonable agreement with OPED (<20% RMS) within the usual range for the pi-meson interactions (~0.3 fm to ~2.5 fm) – in the left curve. Here, OPED (*Y-mod* on the plot) has a spring-like oscillation that is pegged at the lower end, and, stretched and damped as r increases (a behavior well matched by V_{FRACEP}).

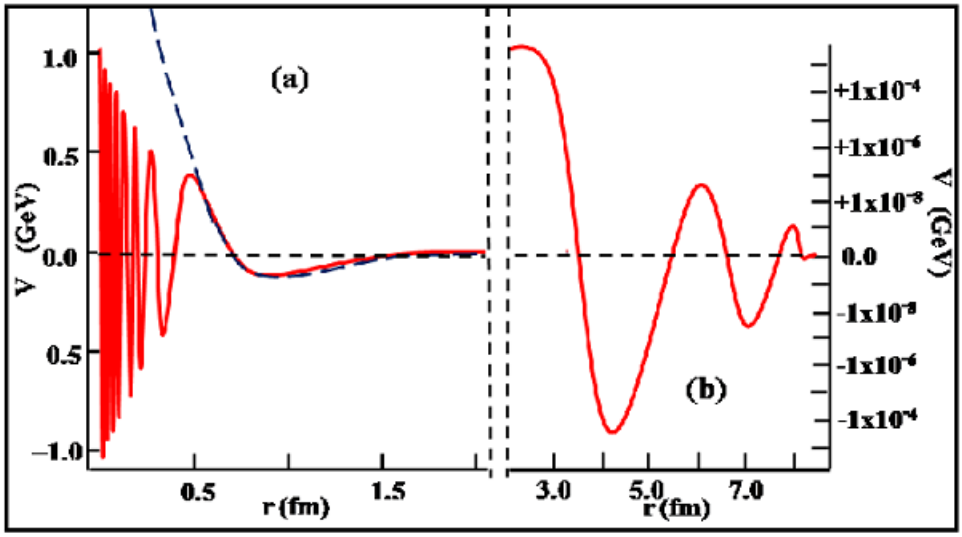

FIGURE 3. Shown is the characteristic behavior at the quantum scale. The solid red line is V_U and the broken blue line is $V_{Y\text{-}mod}$. There are no values for $V_{Y\text{-}mod}$ in the lower (smaller r, near-field) or upper (larger r, far-field) tail regions. The r-values between ~0.5 and 2.0 are the usual values for $V_{Y\text{-}mod}$ for the pi-meson interaction ranges. The V_U's near-field oscillation ($r < 0.25$) approaches its maximum amplitude ($\pm$1.234 GeV) where $V_{Y\text{-}mod}$ increases exponentially. The V_U's damped oscillation in the far-field ($r > 2.5$) is shown on an exaggerated scale. ($m_s = m_t = m_\pi$).

Figure 4 shows the corresponding behavior for the negative pi-meson source. The oscillation amplitude for the leading tail (a), corresponding to the very near-field in the left plot in Fig. 3, has increased so rapidly that there is no obvious oscillation at the smallest r where both the real and imaginary parts increase exponentially due to the hyperbolic sine and hyperbolic cosine functions.

With decreasing r below ~0.5 fm, V_{FRACEP} remains finite – oscillating with increasing frequency as it approaches maximum amplitude of ~1.234 GeV. For $r \geq 2$ in the right curve where OPED is not valid, the oscillating tail exponentially decreases. This is characteristic for all sources to the smallest mass.

For the real part, the potential is positive and repulsive, while the imaginary part is negative and attractive. As r increases to the far-field, corresponding to the right plot in Fig. 3, the oscillating tail exponentially decays. Like the macro-scale cases, the real and imaginary parts are not synchronized and are often out of phase. The transition region between near and far field is so narrow that it is not shown here. (OPED does not address negative mass).

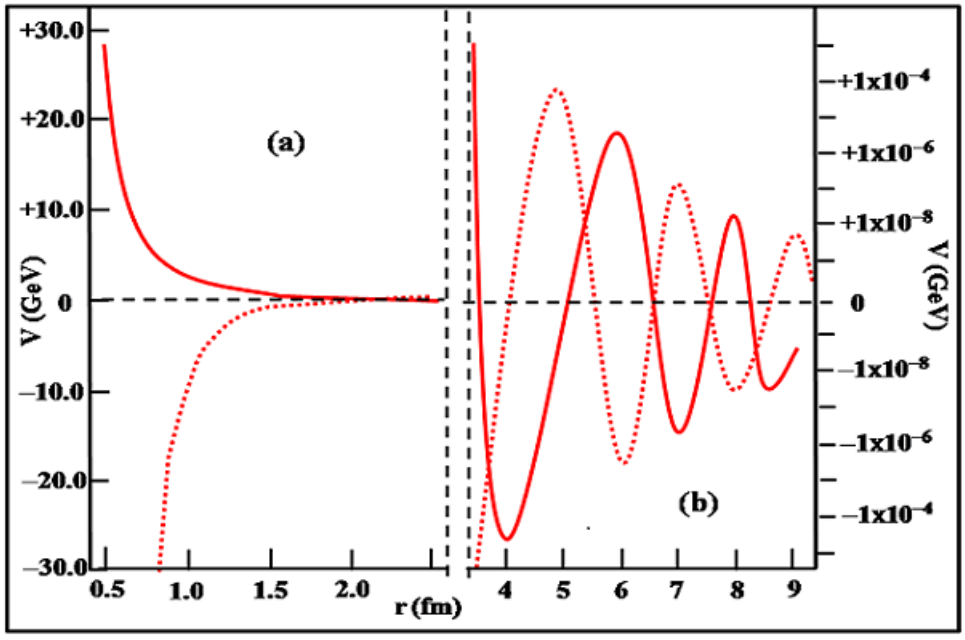

FIGURE 4. Shown is the characteristic behavior at the quantum scale for negative mass sources. The solid red line is the real part, V_{FRACEP}-R; and the dotted red line is the imaginary part, V_{FRACEP}-I. In (a), for r where the OPED model is valid for $+m_\pi$, both V_{FRACEP}-R and V_{FRACEP}-I show no oscillation at smaller r. In this case, V_{FRACEP}-R is repulsive while V_{FRACEP}-I is attractive before going into the larger r oscillation (b), similar to the $+m_\pi$case. ($m_s = -m_\pi = -139.57$ MeV/c^2 and $m_t = +m_\pi$).

5. Conclusions

This effort produced a unified potential (V_{FRACEP}) that characterizes quantum scales through macro and cosmic scales. As developed, it was not intended to provide a model of specific phenomena – only an operational characterization of the overall field behavior – for both positive m_s and negative m_s.

The existence of negative mass is an integral part of V_{FRACEP}. The ultimate goal of this work is a description of the fundamental scales relevant to the composite particles of the FRACEP model which includes both positive and negative mass elements. The imaginary part of the negative-mass characterization in V_{FRACEP} comes from the terms with the square-root of the source mass – an effect not found in V_N or OPED. An intuitive concept for negative mass (and the imaginary part of its potential is uncertain at this time).

At quantum scales for $M > 0$, V_{FRACEP} agrees reasonably well with OPED within the accepted valid range. For $M < 0$, V_{FRACEP} seems to imply any negative m_s interaction is maintained at a much greater distance than observed for positive m_s. The implications of this have not been determined.

One possible point of interest comes from the work of Hoyle, et al. in their development of a canonical form of gravity equations that reduce to General Relativity under certain conditions [27. Their theory indicates that during a creation event (like the Big Bang), pairs of particles, one with both positive mass and the other with negative mass, are created with negative energies ~6×10^{18} GeV.

Both the real and imaginary parts of V_{FRACEP} for $m_s = \mathcal{G}n$ have approximately that magnitude at $r \sim 3 \times 10^{-20}$ fm. This might imply that a pair of particles is created approximately in contact (since the classical radius of the two particles is approximately 3×10^{-20} fm), and, there is an explosive repulsive force between them at that time. One might speculate that the explosive force (driven by the repulsive potential – maybe the initial Dark Energy) is what fed

the initial expansion of the universe at the moment of the Big Bang. Further investigation of this possibility is needed.

At macro scales, for $M > 0$, V_{FRACEP} leads to an attractive potential that agrees with V_N to <0.001% in the "main region" before going into the oscillatory behavior at smaller r that could be interpreted as quantum-like effects around otherwise macro-scale or cosmic-scale sources. For $M < 0$, the real part of V_{FRACEP} leads to a repulsive force (like V_N). The corresponding imaginary part is attractive, and, both parts oscillate (unlike V_N which does not). The full implications of this behavior, relative to cosmological dark matter, have yet to be determined.

Bright matter (positive mass baryons) constitutes <5% of all of the matter/energy in the universe. Dark matter (non-baryonic particles) and dark energy compose the rest. Models generally assume V_N behavior with luminous matter; but, galactic dynamics and other measures indicate there is not enough matter to account for the observations. The search for positive-mass non-traditional matter or modified Newtonian dynamics has not given completely satisfying answers to the dilemma.

This work shows there is a possibility that the $1/r$-Newtonian potential might represent a first order approximation to a more complicated function that unifies all the scales. V_{FRACEP} has characteristic behavior that is consistent with bright matter (positive mass) observations. But, it also allows for the characterization of non-traditional (negative mass) matter that may illuminate the puzzle of dark matter and energy – possibly including things like dark halos around galaxies and the expansion characteristic of the universe.

References

[1] Lao Tzu, trans. Gia-Fu Feng and Jane English. "Verse 1". In *Tao Te Ching*; Vantage Books: NY, USA, verse 1, **1972**.

[2]] I. Newton. “Rules for the Study of Natural Philosophy”. In *The Principia, Book 3,* trans. B. Cohn and A. Whitmann; U. California Press: Berkley, USA, **1999**.

[3] S. Perlmutter et al., “Measurements of the Cosmological Parameters Ω and Λ from the First Seven Supernovae at z ≥ 0.35”. *Astrophys. J.*, 483 (**1997**): 565-581.

[4] R.P. Kirshner, “Throwing Light on Dark Energy”. *Science*, 300 (**2003**): 1914-1918.

[5] F. Zwicky, “On the Masses of Nebulae and of Clusters of Nebulae”. *Astrophys. J.*, 86 (**1937**): 217-246.

[6] G. Burbidge, “On the Masses and Relative Velocities of Galaxies”. *Astrophys. J.*, 196 (**1975**): L7-L10.

[7] M. Milgram, “A Modification of the Newtonian Dynamics as a Possible Alternative to the Hidden Mass Hypothesis”. *Astrophys. J.*, 270 (**1983**): 365-371.

[8] B.A. Dobrescu and D. Lincoln, “Mystery of the Cosmos”. *Sci. Am.*, July (**2015**): 32-39.

[9] J.P. Ostriker and P. Steinhardt, “New Light on Dark Matter”. *Science*, 300 (**2003**): 1909-1913.

[10] A. Cho, “Crunch Time for Dark Matter Hunt”. *Science*, 351 (**2016**): 1376-1377.

[11] E.D. Kovetz, “Probing Primordial-Black-Hole Dark Matter with Gravitational Waves”. *arXiv:1705.09182v2* , (**2017**).

[12] S. Bird et al., “Did LIGO Detect Dark Matter?”. *Phys. Rev. Lett.*, 116 (**2016**) 201301.

[13] J.L. Feng, “Dark Matter at the Fermi Scales”. *arXiv:astro-ph/0511043v1*, (**2005**).

[14] J. Kumar and J.L. Feng, “WIMPless Dark Matter”. *arXiv:0909.2877v1*, (**2009**).

[15] G. Chardin and G Manfredi, “Gravity, Antimatter and the Dirac-Milne Universe”. *Hyperfine Interactions*, 239 (**2018**): 45 (15 pages).

[16] K. Barghout, “Analysis of Repulsive Central Force Field on Solar and Galactic Dynamics”. *Open Phys.*, 17 (**2019**): 364-372.

[17] K. Barghout, “MLG vs. MOND”. *J. Mod. Phys.*, 6 (**2015**): 490-495.

[18] Yi-Fang Chang, “Field Equations of Repulsion Force between Positive-Negative Matter, Inflation Cosmos and Many Worlds”. *Int. J. Mod. Theoretical Phys.*, 2 (**2013**): 100-117.

[19] Yi-Fang Chang, “Astronomy, Black Hole and Cosmology on Negative Matter, and Qualitative Analysis Theory”. *Int. J. Mod. Applied Phys.*, 4(2) (**2014**): 69-82.

[20] Yi-Fang Chang, “Negative Matter as Dark Matter, and Its Judgment Test and Calculation of Ratio”. *Int. J. Mod. Applied Phys.*, 9(1) (**2019**): 1-12.

[21] J.P. Petit and G. D’Agostini, “Cosmological Bimetric Model with Interacting Positive and Negative Masses and Two Different Speeds of Light, in Agreement with the Observed Acceleration of the Universe”. *Mod. Phys. Lett.* A29 (**2014**) 1450182 (15 pages).

[22] J.P. Petit and G. D’Agostini, “Negative Mass Hypothesis in Cosmology and the Nature of Dark Energyl”. *Astrophys. Space Sci.* 1 (**2014**) 45 (5 pages).

[23] J. Giannini, "Fractal Composite Quarks and Leptons with Positive and Negative Mass”. *Int. J. Mod. Theoretical Phys.*, 8 (**2019**): 41-63.

[24] C.A. Bertulani. “The Nucleon-Nucleon Interaction”. In *Nuclear Physics in a Nutshell*; Princeton U. Press: Princeton, NJ, 71-97, **2007**.

[25] J.A. Giannini, “Feasibility of Constructing a Unified Positive and Negative Mass Potential”. *Int. J. Mod. Theoretical Phys.*, 8 (**2019**): 1-16.

[26] V is plotted in log-log format as the sign of V times the ln|V|. In the oscillatory region where V crosses from positive to negative values, the natural log introduces an artificial exponential growth to a singularity (between $V < -1$ and $V > +1$) that does not reflect the actual potential behavior. To address this and more properly reflect the behavior of V_{FRACEP},

the plot smoothly connects the two non-oscillatory regions on either side of the area in question.

[27] F. Hoyle, G. Burbidge, and J.V. Narlikai. “A Summary of the Material Contained in the Previous Chapters”. *A Different Approach to Cosmology*; Cambridge U. Press: Cambridge, UK, pp. 311-320, **2000**.